RESEARCH REPORT

Unclassified

Security Classification

DOCUMENT CONTROL DATA - R & D

Security classification of title, body of abstract and indexing annotation must be entered when the overall report is classified

1. ORIGINATING ACTIVITY (Corporate author)	2a. REPORT SECURITY CLASSIFICATION
Battelle, Columbus Laboratories 505 King Avenue Columbus, Ohio 43201	2b. GROUP

3. REPORT TITLE

Influence of Microstructure on Fracture Propagation in Rock

4. DESCRIPTIVE NOTES (Type of report and inclusive dates)

Semiannual Technical for period December 17, 1970 to June 30, 1971

5. AUTHOR(S) (First name, middle initial, last name)

Richard G. Hoagland, George T. Hahn, and Alan R. Rosenfield

6. REPORT DATE	7a. TOTAL NO. OF PAGES	7b. NO. OF REFS
August 3, 1971	38	9

8a. CONTRACT OR GRANT NO.	9a. ORIGINATOR'S REPORT NUMBER(S)
H0210006 b. PROJECT NO.	None
c. d.	9b. OTHER REPORT NO(S) (Any other numbers that may be assigned this report) None

10. DISTRIBUTION STATEMENT

Unrestricted

11. SUPPLEMENTARY NOTES	12. SPONSORING MILITARY ACTIVITY
	Advanced Research Project Agency

13. ABSTRACT

This report describes the results of research in progress to correlate the fracture resistance with microstructural features of Salem limestone and Berea sandstone. These tests are being conducted on wedge-loaded double-cantilever-beam specimens. The fracture resistance of Salem limestone measured in terms of R, the energy dissipation rate, was found to be strongly dependent on the crack orientation with respect to the bedding plane and ranges from about 40 joules/m^2 to 220 joules/m^2. During these tests, acoustic emission from the rock specimens are monitored to detect the onset of cracking. The value of R for the sandstone is approximately the same as for the limestone, although the extreme nonlinear behavior of the material has so far prevented a more definitive measurement. The mode of fracture and fracture path in both materials has been identified by fractography over a broad range of magnifications. A comparison of the R values and their meaning in terms of strength predictions is made with data obtained by other means. Consideration of these results leads to a model of fracture in these two materials involving the development of extensive microcracking in the region surrounding the main crack tip.

DD FORM 1473

Unclassified

Security Classification

14 KEY WORDS	LINK A		LINK B		LINK C	
	ROLE	WT	ROLE	WT	ROLE	WT
Limestone						
Sandstone						
Fracture Mechanics						
Fracture Resistance						
Microstructure						
Strength						
Acoustic Emission						

SEMIANNUAL REPORT

on

INFLUENCE OF MICROSTRUCTURE ON FRACTURE PROPAGATION IN ROCK

by

R. G. Hoagland†, G. T. Hahn††, and A. R. Rosenfield†

Contract H0210006

Effective December 18, 1970
Expires December 18, 1971

Amount of Contract $42,150

Sponsored by
Advanced Research Projects Agency
ARPA Order No. 1579, Amend. No. 2
Program Code No. 1F10

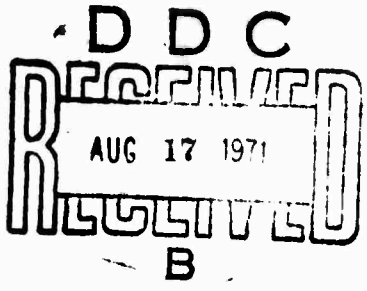

BATTELLE
Columbus Laboratories
505 King Avenue
Columbus, Ohio 43201
Phone: 614-299-3151

† Project Scientists
†† Principal Investigator

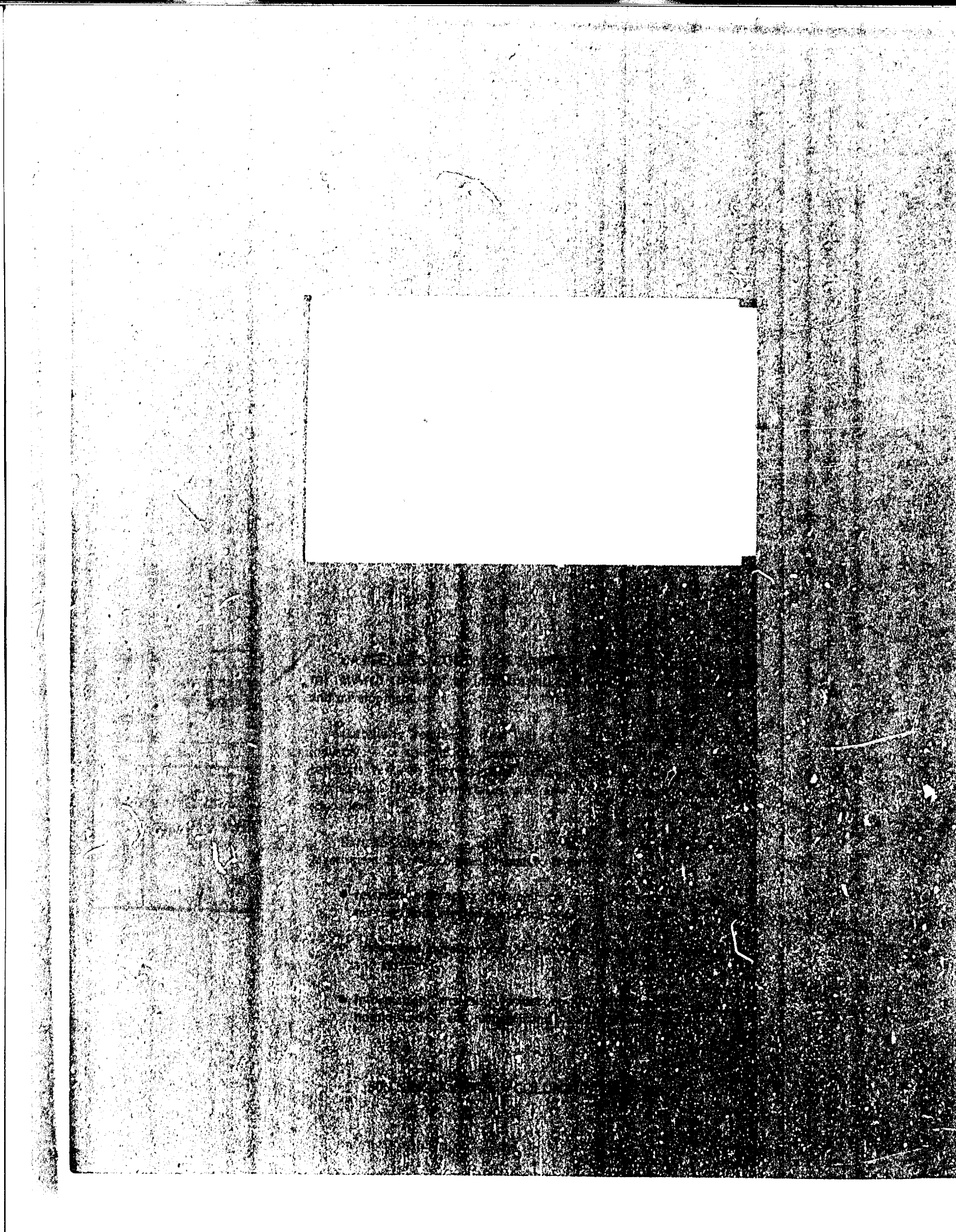

SEMIANNUAL REPORT

on

INFLUENCE OF MICROSTRUCTURE ON FRACTURE PROPAGATION IN ROCK

to

BUREAU OF MINES
TWIN CITIES RESEARCH CENTER

August 3, 1971

by

R. G. Hoagland, G. T. Hahn, and A. R. Rosenfield

BATTELLE
Columbus Laboratories
505 King Avenue
Columbus, Ohio 43201

NOTICE TO USERS

Portions of this document have been judged by the NTIS to be of poor reproduction quality and not fully legible. However, in an effort to make as much information as possible available to the public, the NTIS sells this document with the understanding that if the user is not satisfied, the document may be returned for refund.

If you return this document, please include this notice together with the IBM order card (label) to:

National Technical Information Service
U.S. Department of Commerce
Attn: 952.12
Springfield, Virginia 22151

SUMMARY

This report describes the results of research in progress to correlate the fracture resistance with microstructural features of Salem limestone and Berea sandstone. These tests are being conducted on wedge-loaded double-cantilever-beam specimens. The fracture resistance of Salem limestone measured in terms of R, the energy dissipation rate, was found to be strongly dependent on the crack orientation with respect to the bedding plane and ranges from about 40 joules/m^2 to 220 joules/m^2. During these tests, acoustic emission from the rock specimens are monitored to detect the onset of cracking. The value of R for the sandstone is approximately the same as for the limestone, although the extreme nonlinear behavior of the material has so far prevented a more definitive measurement. The mode of fracture and fracture path in both materials has been identified by fractography over a broad range of magnifications. A comparison of the R values and their meaning in terms of strength predictions is made with data obtained by other means. Consideration of these results leads to a model of fracture in these two materials involving the development of extensive micro-cracking in the region surrounding the main crack tip.

SEMIANNUAL REPORT

on

INFLUENCE OF MICROSTRUCTURE ON FRACTURE PROPAGATION IN ROCK

by

R. G. Hoagland, G. T. Hahn, and A. R. Rosenfield

INTRODUCTION

The microstructural properties of rocks are in many ways more complex than other engineering materials such as metals. They are typically much more discontinuous due to the presence of voids, cracks, or planes of weakness and often contain a number of phases with various crystallographic symmetries. For these reasons there is a considerably larger body of information relating the important mechanical properties of metals to microstructure than exists for rocks. One example of special importance is the response to a tensile stress. In the final stages of plastic straining of a metal, voids or cracks form at inhomogeneities which grow and coalesce leading finally to fracture. If, on the other hand, the metal contains a preexisting crack, plastic flow begins at much lower loads but is confined to the region of high stresses at the crack tip. This region can tolerate stresses or strains to an extent characteristic of the material before the crack begins to extend and fracture occurs. This tolerance limit can be established in terms of the parameter, R, the energy dissipated per unit area of crack surface formed as the crack begins to grow. Using R and the concepts embodied in fracture mechanics, one can predict, for a given structure, the combination of flaw size and applied load which will produce failure. Research into the microstructural origins of R in metals has also been fairly successful in discovering those microstructural features of metals which are most important to the fracture resistance.

Can the microstructure of rocks be related to their resistance to crack propagation with at least the same degree of success as in the case of metals? This program is investigating this aspect of rock mechanics through a series of experiments to measure R together with high-resolution fractography and petrography. The research this year is aimed at three esentially monomineralic rocks: Salem limestone, Sioux quartzite, and Berea sandstone. The report describes the results of fairly extensive tests which so far have been conducted on Salem limestone and also some results obtained on Berea sandstone, although the latter is yet incomplete.

Salem Limestone†

Energetics of Fracture

The energy dissipation rates for relatively slow, stable crack extension have been measured by means of the double-cantilever-beam (DCB) test specimen and loading arrangement shown in Figure 1. The specimen dimensions are 1.6 x 7.6 x 17.8 cm with a 0.4 mm-wide sawcut placed to facilitate starting a crack having the desired orientation*. Prior to testing, the specimens were baked at 110°C in order to minimize differences in moisture content from one specimen to another. The effect of moisture content has not yet been established but may be important. To measure the growth of the crack a parallel array of conductive lines is placed on the specimen. The electrical resistance of the array is monitored during testing and, as the crack severs the lines, the corresponding resistance change reveals the crack-tip location. Because of the relative brittleness of the rock, some difficulty was encountered in finding a sufficiently brittle material for the conductive stripes which fail

---

† Salem, Indiana, and Bedford are equivalent designations for this limestone.

* Orientations are relative to the bedding plane.

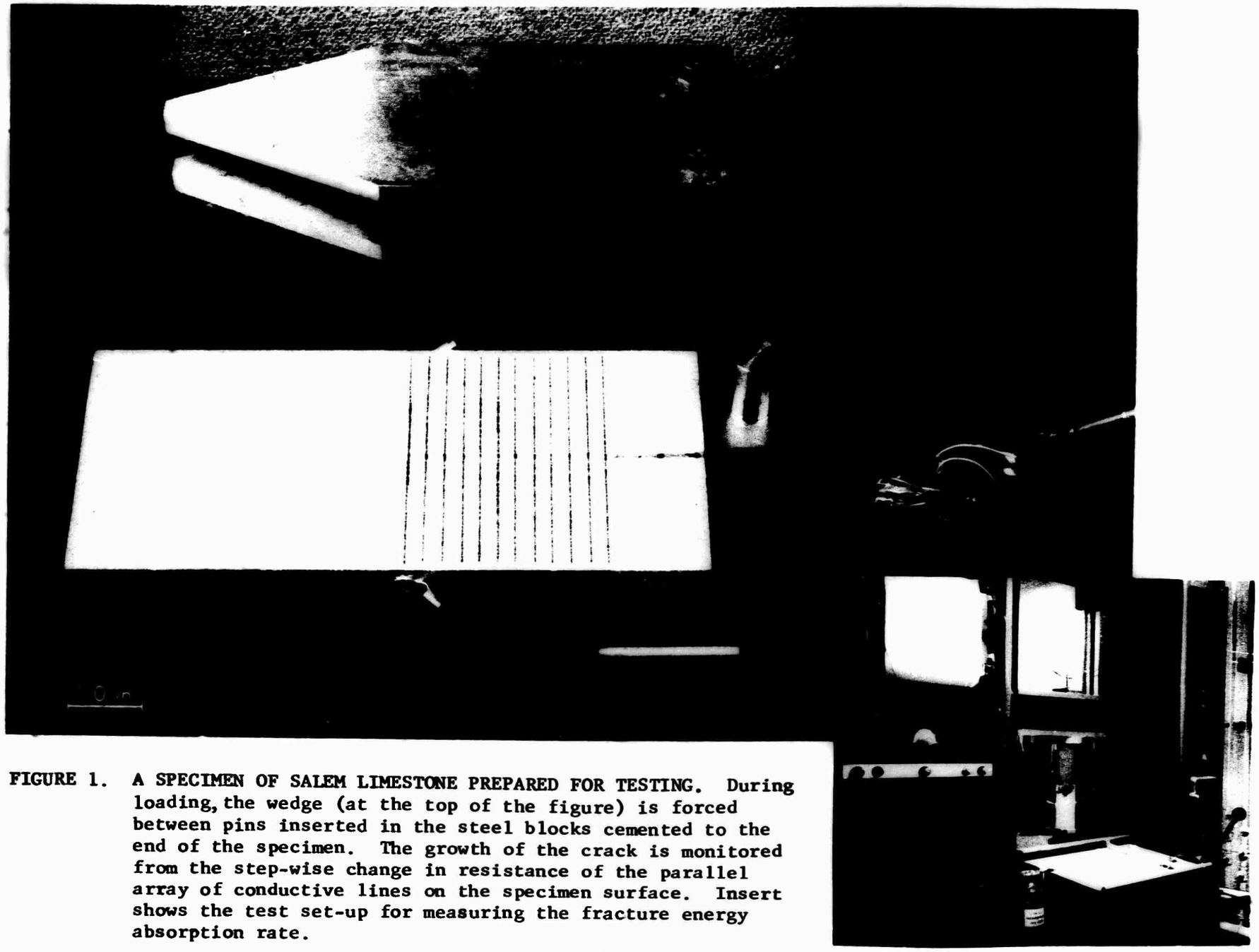

FIGURE 1. A SPECIMEN OF SALEM LIMESTONE PREPARED FOR TESTING. During loading, the wedge (at the top of the figure) is forced between pins inserted in the steel blocks cemented to the end of the specimen. The growth of the crack is monitored from the step-wise change in resistance of the parallel array of conductive lines on the specimen surface. Insert shows the test set-up for measuring the fracture energy absorption rate.

reproducibly the instant the crack in the rock passes through. Lines drawn on the surface with a lead pencil were found to be more reliable than either silver paint or a number of vapor deposited metals, although some uncertainty in the crack length measurements remains.

During testing, a wedge is forced between a pair of steel pins located in either side of the specimen and the resulting opening of the crack is measured with a displacement gage (c.f. Figure 1 insert). A typical test record of the load applied to the wedge and the resulting crack opening displacement for a specimen of Salem limestone is shown in Figure 2. The initial part of the load-displacement record is linear indicating a purely elastic behavior. Above about 75 lbs the record becomes increasing nonlinear. This nonlinearity is the result of either the beginning of crack extension from the slot tip or the development of some inelastic process in the region of high stresses surrounding the notch.

Typically, no crack estension is indicated initially by the conductive strips or by optical observations of 20x magnifications, although these indications may not be reliable because of extremely small crack opening displacements. Recently, evidence of cracking occurring at relatively low applied loads was obtained from acoustic emission measurements. These measurements were made by attaching piezoelectric crystals to the specimen surface. The crystals were acoustically coupled to the specimen by means of a viscous resin. The crystals have a resonant frequency of 150 kHz and, therefore, it is this frequency of acoustic pulses which is most sensitively detected. In tests monitoring acoustic emissions, the specimens were placed on a rubber pad on the loading platen and teflon sheets were used between the wedge and pins. These precautions were aimed at minimizing the stray noise from specimen-platen contact or from sliding of the wedge along the pin. Tests on uncracked specimens showed that these

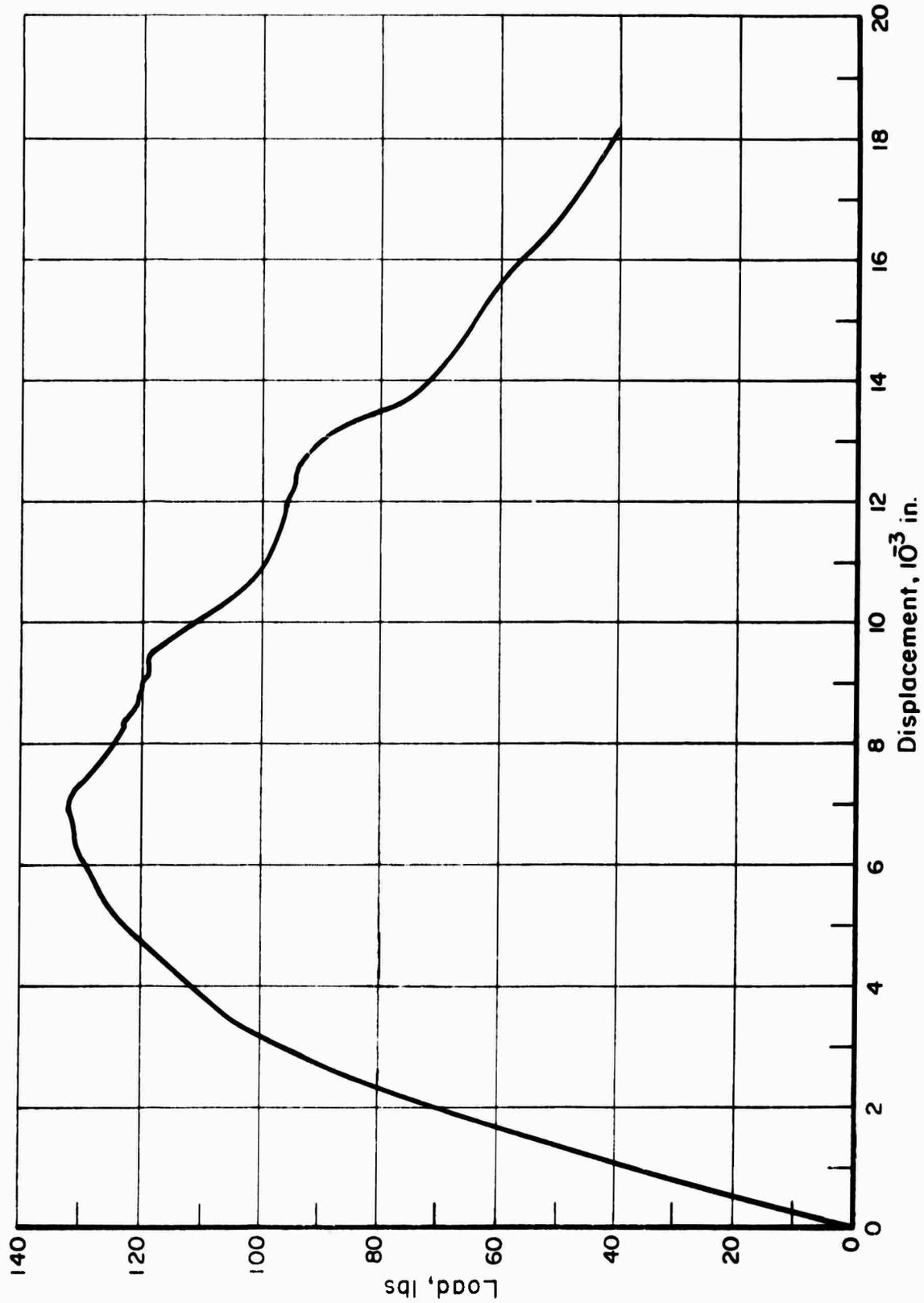

FIGURE 2. A TYPICAL LOAD-DISPLACEMENT RECORD FROM A WEDGE-LOADED DCB TEST. In the initial part of the record the crack has not yet begun to grow as indicated by the linear relation between the load and displacement. In the latter part, the load is gradually decreasing as the crack extends at a more or less constant rate.

precautions were effective, and, therefore, acoustic pulses registered by the recording equipment during an actual test originate in the bulk of the specimen, presumably in the region of high stress surrounding the slot tip. Figure 3 shows an example of the acoustic emission rate (counts/minute) correlated against applied load. Significant acoustic activity, which quite likely derives from cracking, is detected at loads even below those at which a nonlinearity is evident in the load-displacement record. This evidence coupled with other results described below points to the development of numerous cracks in the volume surrounding the slot tip which may, as a result, account for the gradual decrease in slope in the early stages of the test. The advance of the crosshead was also stopped several times during this test and in others. Upon stopping the crosshead advance the acoustic activity did not terminate immediately, but instead the count rate decayed gradually as did the load indicateing some additional growth of the crack. This behavior of crack growth under fixed displacement conditions is often observed in metals and is referred to as subcritical cracking. Generally, it is associated with a reaction between the environment and the exposed surface at or very near the tip of the crack. The possibility that cracks can grow through statically loaded limestone as a result of attack by agents in the air (e.g., water vapor) seems a plausible explanation of these results although more work into this behavior would be required for verification.

Generally at the maximum load, the growth of the main crack, slowly extending from the slot tip, is clearly evident. The rate of advance of the crack is stable†, i.e., it is controlled by the rate of advance of the wedge.

---

† Experiments are in progress in which the energy dissipation rate of rapidly moving cracks is being measured.

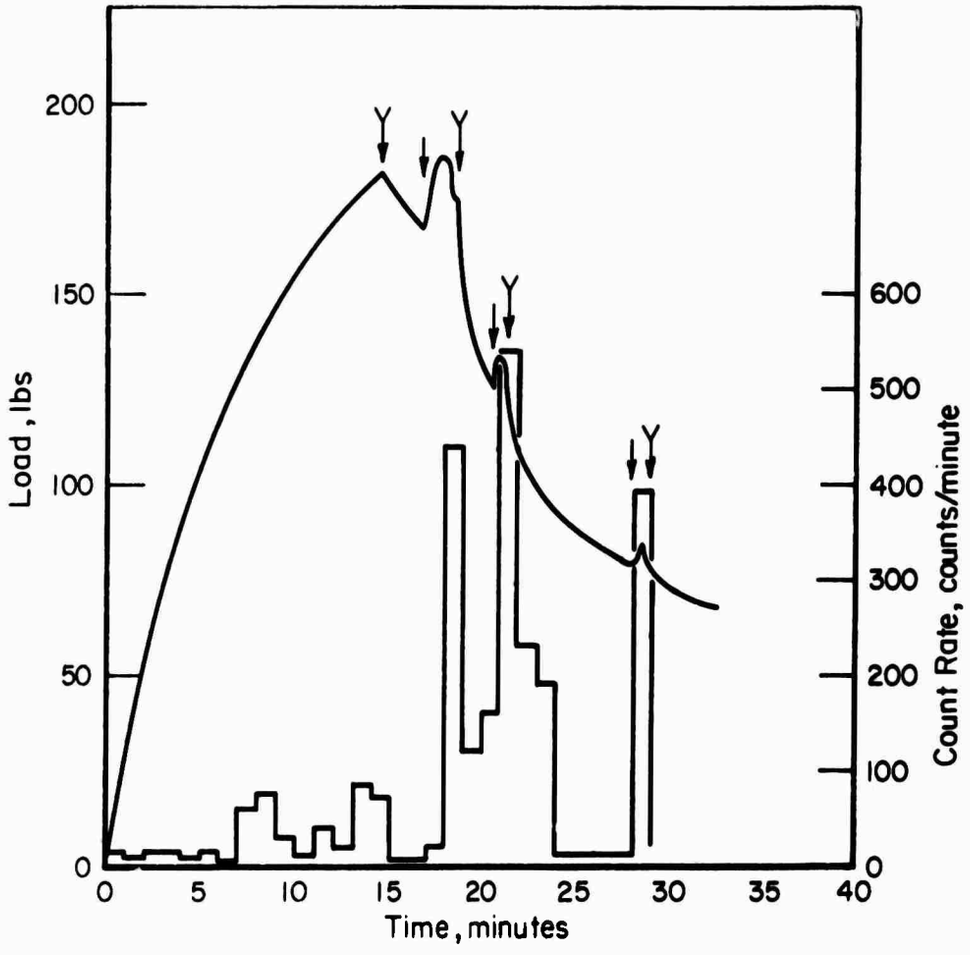

FIGURE 3. AN EXAMPLE OF THE RATE OF ACOUSTIC PULSES RECEIVED DURING TESTING OF A SALEM LIMESTONE SPECIMEN. The count rate is correlated with the wedging load applied to the specimen. The noise or background level is approximately 30 counts/minute. The cross-head advance of the testing machine was stopped at the time designated by the double-ended arrows and restarted at the single-ended arrows.

Since R is the energy dissipation rate per unit area of crack advance, then

$$R = \frac{d}{dA} (W-U) \qquad (1)$$

where dW represents the work done by the testing machine during an increase of the crack area by dA and dU is the corresponding change in strain energy in the specimen. Equation (1) applies to the case where the crack is growing slowly for which the kinetic energy in the system is negligible. An analysis based on Equation (1) has been developed at Battelle which allows R to be computed from either the load-displacement record or from measured displacements and crack lengths. Details of this analysis are given in the Appendix. By convention, R is based on the projected surface area:

$$dA = bda \qquad (2)$$

where b is the specimen thickness and a is the crack length. As shown in the next section, the actual crack surface is highly irregular, and the true surface area is larger than assumed in calculating R. This is an important consideration in interpreting the results of these tests.

The calculation of R from the load-displacement record involves E, Young's modulus. E was measured for this limestone by determining the slope (compliance) of the load-displacement record for a DCB specimen containing a crack of known length and comparing this value with the modulus independent compliance derived from elasticity theory. The ratio of these two compliances gives the value of E as 1.6×10^{11} dynes/cm^2 (2.3×10^6 psi). This value compares quite well with the zero stress value obtained from uniaxial com-

pression data by Hardy and Kim[1] on similar material. However, the maximum load used in measuring E was small in order to prevent crack extension. Because the limestone behaves as a fairly inelastic material it is possible that the magnitude of E used to calculate R should be less than this. This effect is particularly evident from the tests on the sandstone and an analysis to account for nonlinear behavior is currently under consideration.

A comparison of R for three orientations of cracking in Salem limestone are shown in Figure 4. These preliminary results have been compiled from test records, like that shown in Figure 2, for a range of crack lengths starting from the initial sawcut to a point where the test was either terminated or the crack deviated by more than 0.3 cm from the midplane of the specimen (i.e., from a straight path). Typically, the results show that R increases gradually in the initial stages of crack growth and then attains a relatively constant level. The differences in the value of R associated with the plateau for each of the three orientations points to a significant anisotropy in the resistance to cracking for this material. Fracture on a plane parallel to the bedding plane (AX) is accompanied by the lowest energy absorption rate while cracking on a plane perpendicular to the bedding plane but in a direction parallel to it (CY) requires substantially more energy. Perkins and Bartlett[2] report an energy dissipation rate 84 J/m^2 (0.48 in.-lbs/$in.^2$) for a rock they identify as Indiana limestone†. While they did not report the orientation of their crack plane this value is comparable to but somewhat on the low side of the range of data reported here.

---

† Perkins and Bartlett express their results in terms of surface energy, γ while $R = 2\gamma$. Both R and γ are based on the projected surface area of the crack.

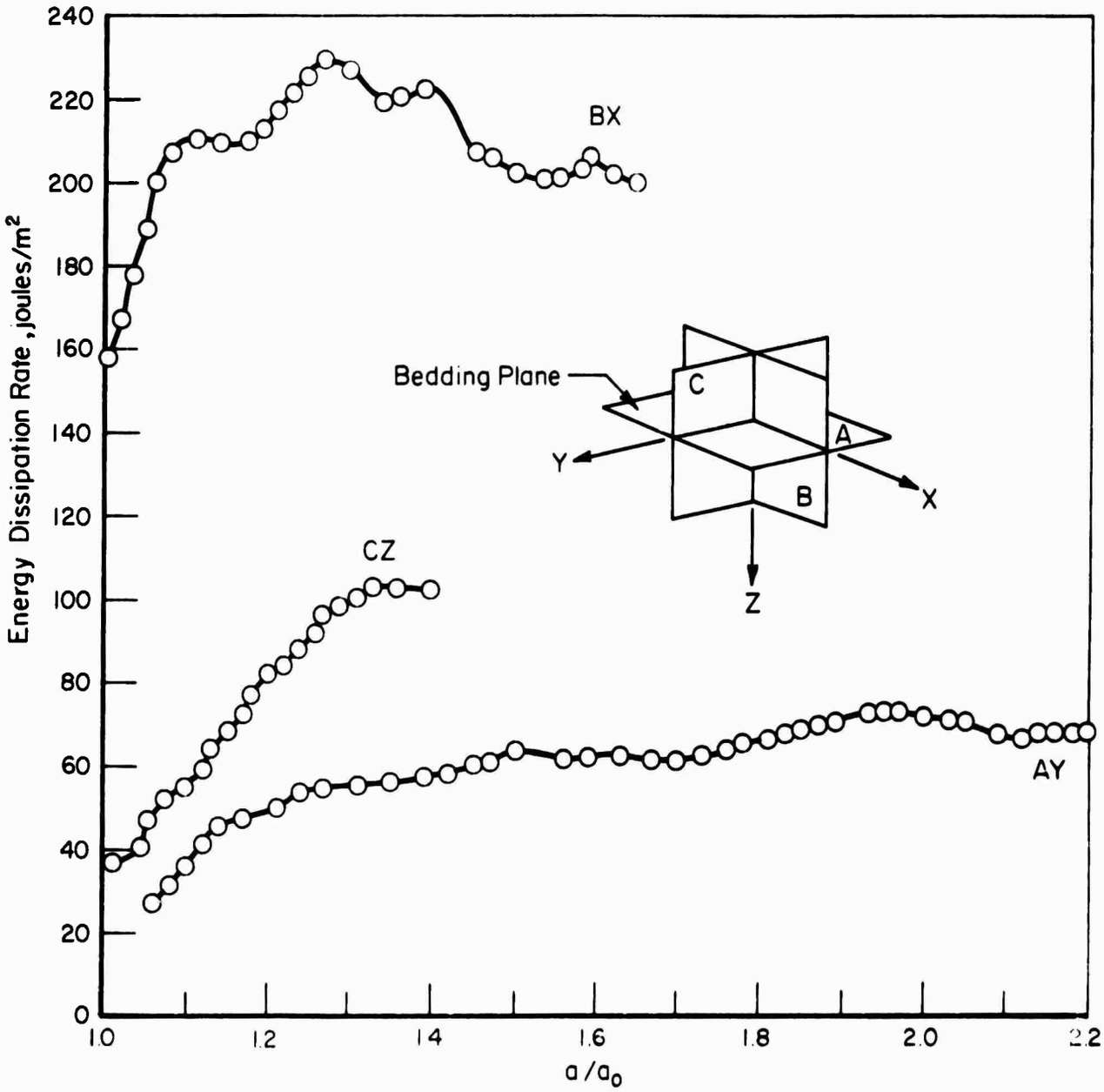

FIGURE 4. ENERGY DISSIPATION RATES MEASURED OVER AN INTERVAL OF CRACK LENGTH FOR THREE ORIENTATIONS OF THE CRACK PLANE AND PROPAGATION DIRECTION IN SALEM LIMESTONE. The letters A, B, and C denote orientation of the crack plane with respect to the bedding plane (plane A) and X, Y, and Z denote crack propagation direction. a/a_o is the ratio of crack length to the starting slot length.

Microstructure

The microstructure of the Salem limestone specimens consists of an aggregate of particles identifiable as calciferous fossils or fragments of fossils together with öolites. The particles are loosely packed and considerable pore space is observable. The diameters of the particles in this aggregate are principally in the range of 0.5 mm to 2.0 mm. At low magnification (~ 30X) the particles appear to be cemented by a white powdery material (the matrix). At higher magnifications the granular character of the matrix is observable as can be seen in Figure 5 which shows electron micrographs of a replica made from a polished and lightly etched surface. Both views in Figure 5 show the structure within the matrix or at the interface of a larger particle (öolite or fossil fragment). The fine particles comprising the matrix appear to have a diameter of about 1 μ. The reflecting optical micrographs in Figure 6 display the heterogeneous nature of the microstructure and also show the path of the crack. The micrographs in Figure 6 were obtained from a polished surface of a specimen with a crack of the AY orientation (see Figure 4). The specimen was first prepared for observation by infiltrating the crack and the interconnecting pores with an epoxy in order to prevent tearing out of loose material during polishing. These micrographs indicate that the crack propagates most often through the matrix described above. There is, however, considerable fracture of the fossil debris and öolites as can be seen in Figure 6b. Note also that because the crack predominantly follows the matrix, the path is highly irregular and, therefore, the actual surface area created during fracturing is larger than the area referred to in Equation (2) and on which the calculation of R is based.

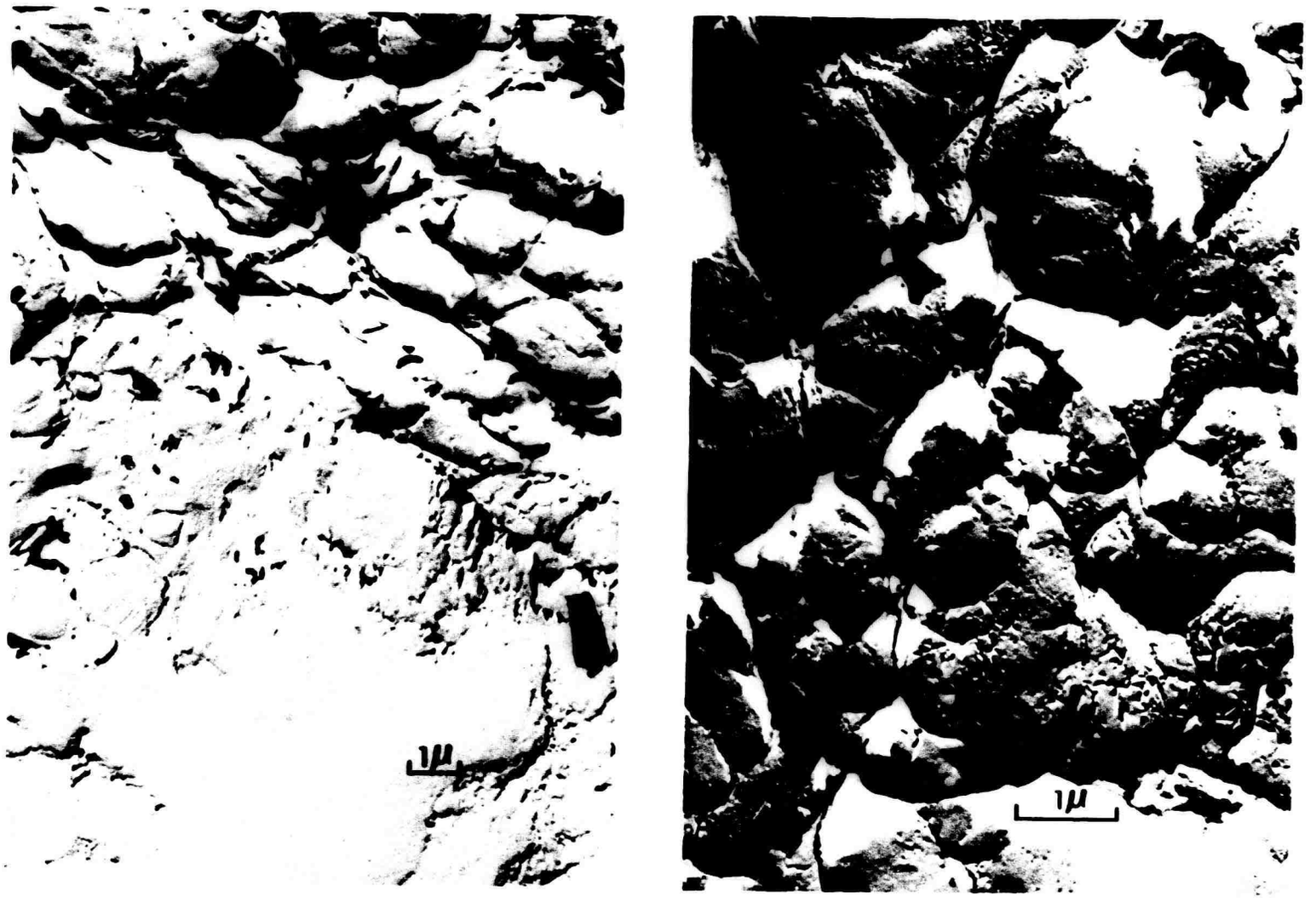

(a) (b)

FIGURE 5. EXAMPLES OF MICROSTRUCTURE REVEALED BY ELECTRON MICROSCOPY OF REPLICAS OF A POLISHED AND ETCHED SURFACE OF INDIANA LIMESTONE (etchant: 50% HF, 50% glacial acetic).

(a)

FIGURE 6. CRACK PROFILES AT THE MIDTHICKNESS PLANE OF A SALEM LIMESTONE SPECIMEN. The specimen has been impregnated with an epoxy resin: (a) region near the initial slot tip and (b) region containing the crack tip.

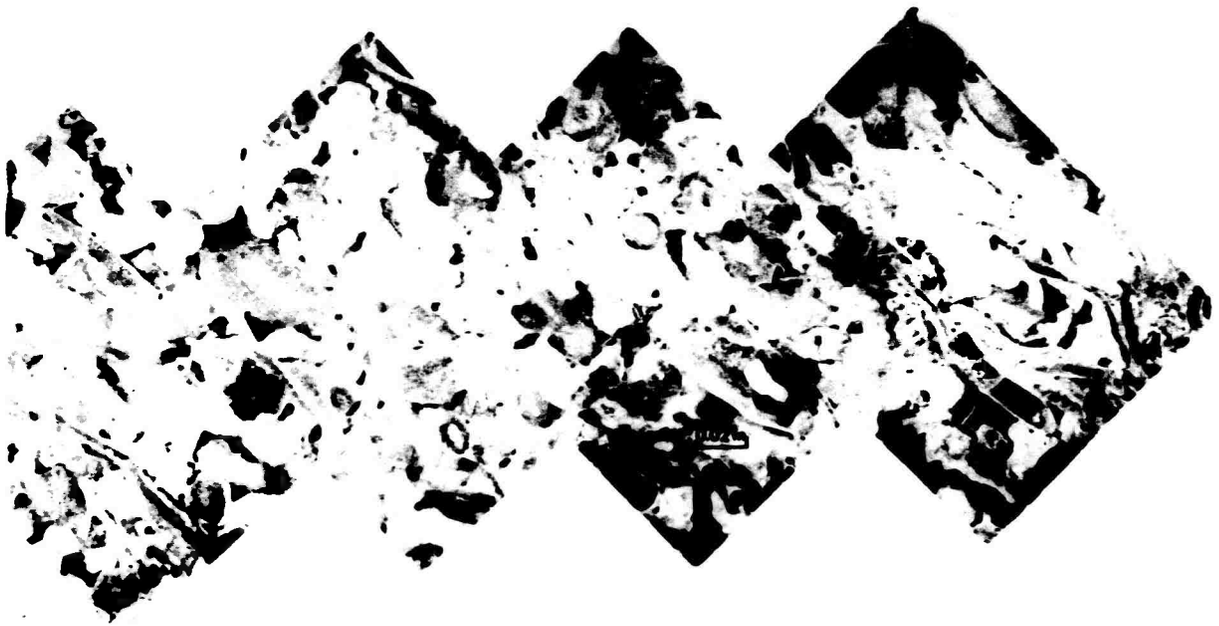

(b)

FIGURE 6. CRACK PROFILES AT THE MIDTHICKNESS PLANE OF A SALEM LIMESTONE SPECIMEN (Continued).

Fractography

Proceeding to higher magnifications of the fracture surface reveals more clearly the highly irregular character of the surface topography. Figures 7a, b, and c are a sequence of stereo pairs† of progressively increasing magnification made by scanning electron microscopy of an area of the fracture surface of a Salem limestone specimen. In Figure 7a the outline of a number of millimeter size particles are observable. Figure 7b reveals an area where the crack has passed partially through the matrix material as well as through larger particles. The fracture surfaces of the larger particles (whether fossil fragments, precipitated crystals, or oölites) display distinct cleavage patterns reminiscent of cleavage of single crystals. Verification that these are single crystals of calcite or at least highly oriented polycrystals is discussed in reference to Figure 8. At high magnification the fine micron size particles comprising the matrix appear to be faceted as shown in Figure 7c which suggests that these also may be single crystals. The utility of the scanning electron microscope derives from the large depth of focus it provides at all levels of magnifications. A good example of this capability is shown in Figure 7d which reveals a pore broken open during fracture and which contains a lining of nearly perfect crystals of calcite or perhaps magnesite.

In order to resolve features as small as 20 angstroms, plastic replicas were made of the fracture surfaces. A platinum-carbon mixture was then vapor deposited onto the plastic replica which, in turn, was then dissolved in acetone. The Pt-C films are placed in an electron microscope in which an electron beam passes through the films and the resulting image can be displayed on a phosphor screen or photographed. During the replication process of the

† A three-dimensional effect is obtained when viewing these micrograph pairs through a stereo viewer. If such a viewer is available the pages should be removed and slit down the center in order to adjust the spacing between the micrographs for the viewer used.

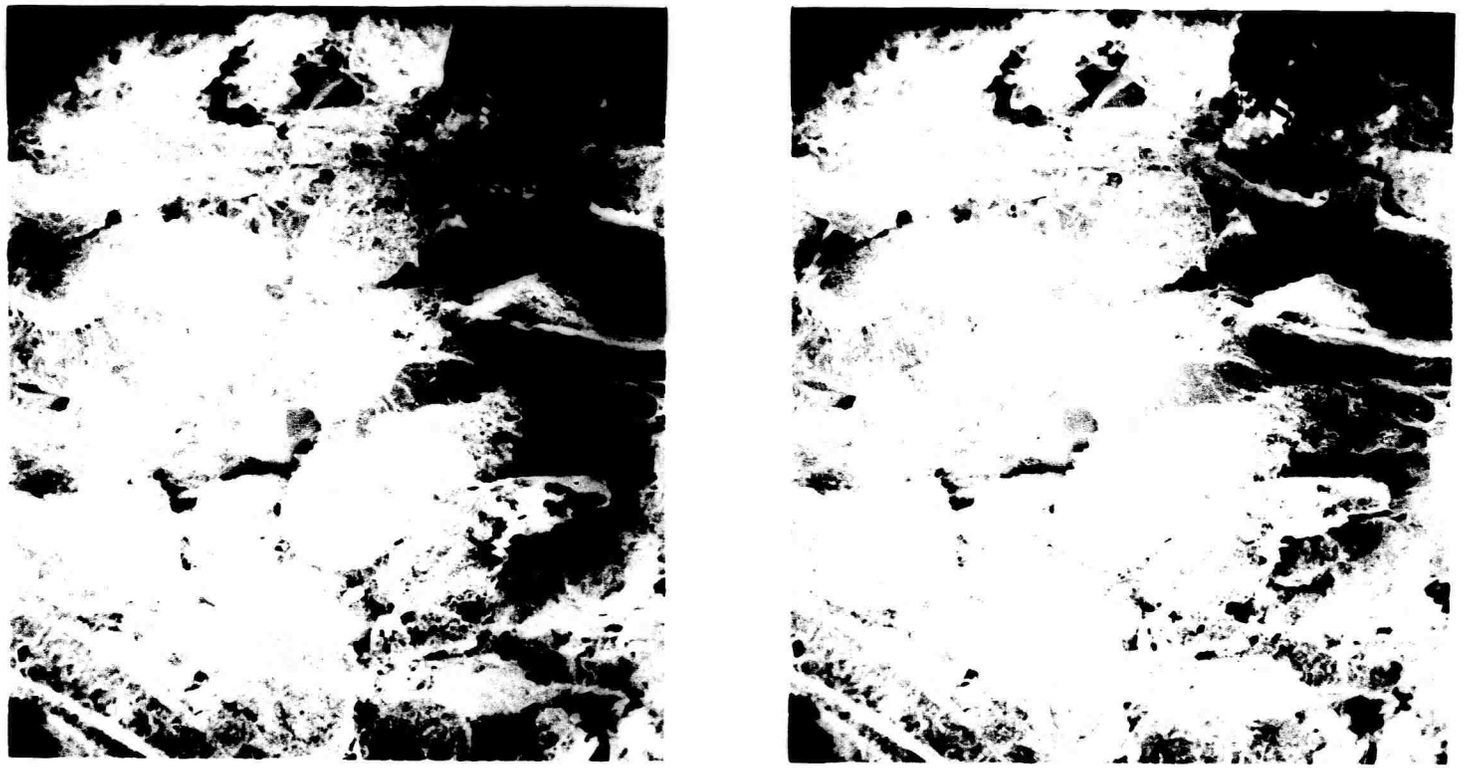

(a) Low magnification view of fracture surface revealing outlines of broken fossils and öolites. (50X)

FIGURE 7. STEREO PAIRS OBTAINED BY SCANNING ELECTRON MICROSCOPY OF FRACTURE SURFACE IN SALEM LIMESTONE.

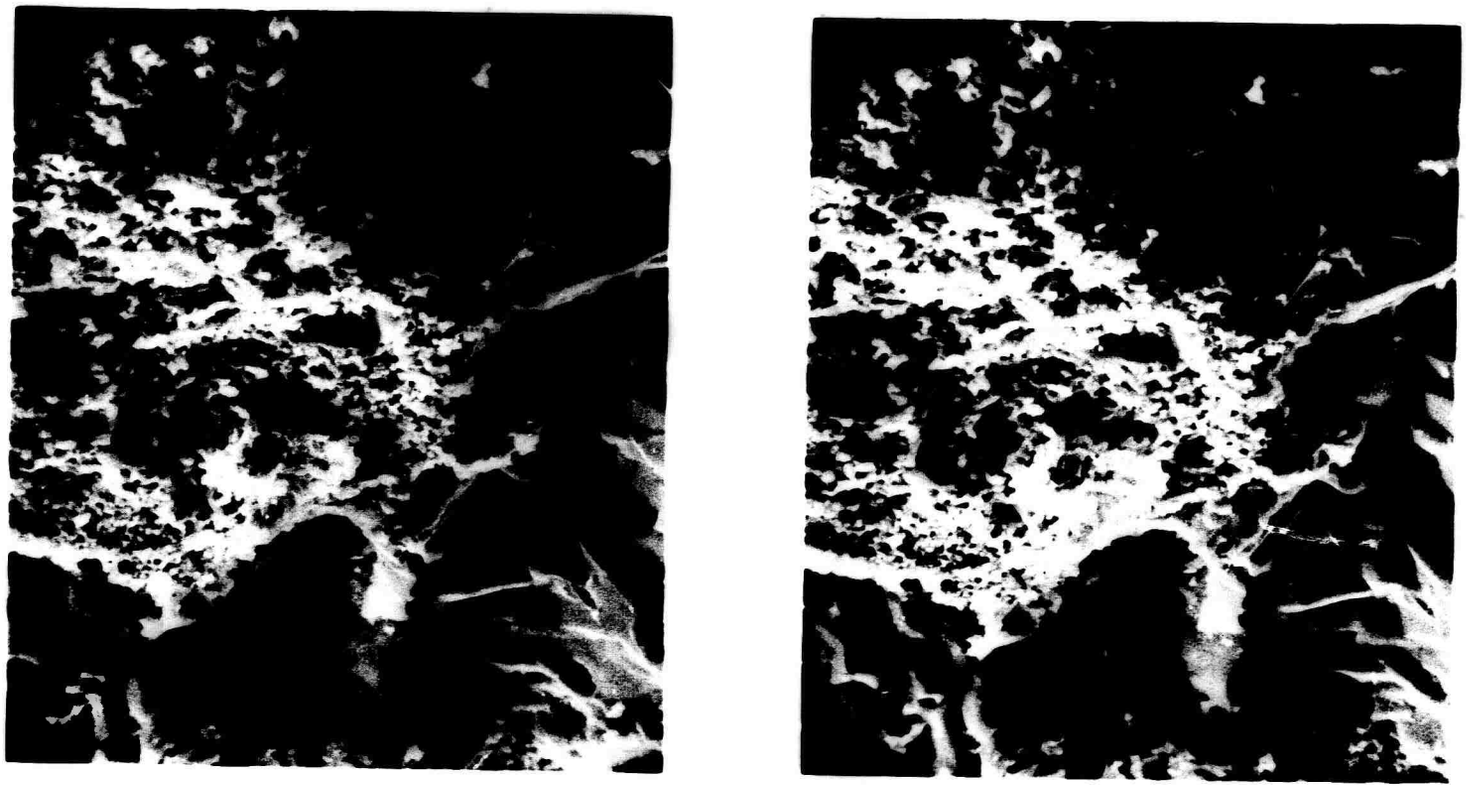

(b) Here the crack has passed partially through the crystalline öolites as well as through the much finer aggregate of particles cemented between the öolites. (500X)

FIGURE 7. STEREO PAIRS OBTAINED BY SCANNING ELECTRON MICROSCOPY OF FRACTURE SURFACE IN SALEM LIMESTONE (Continued).

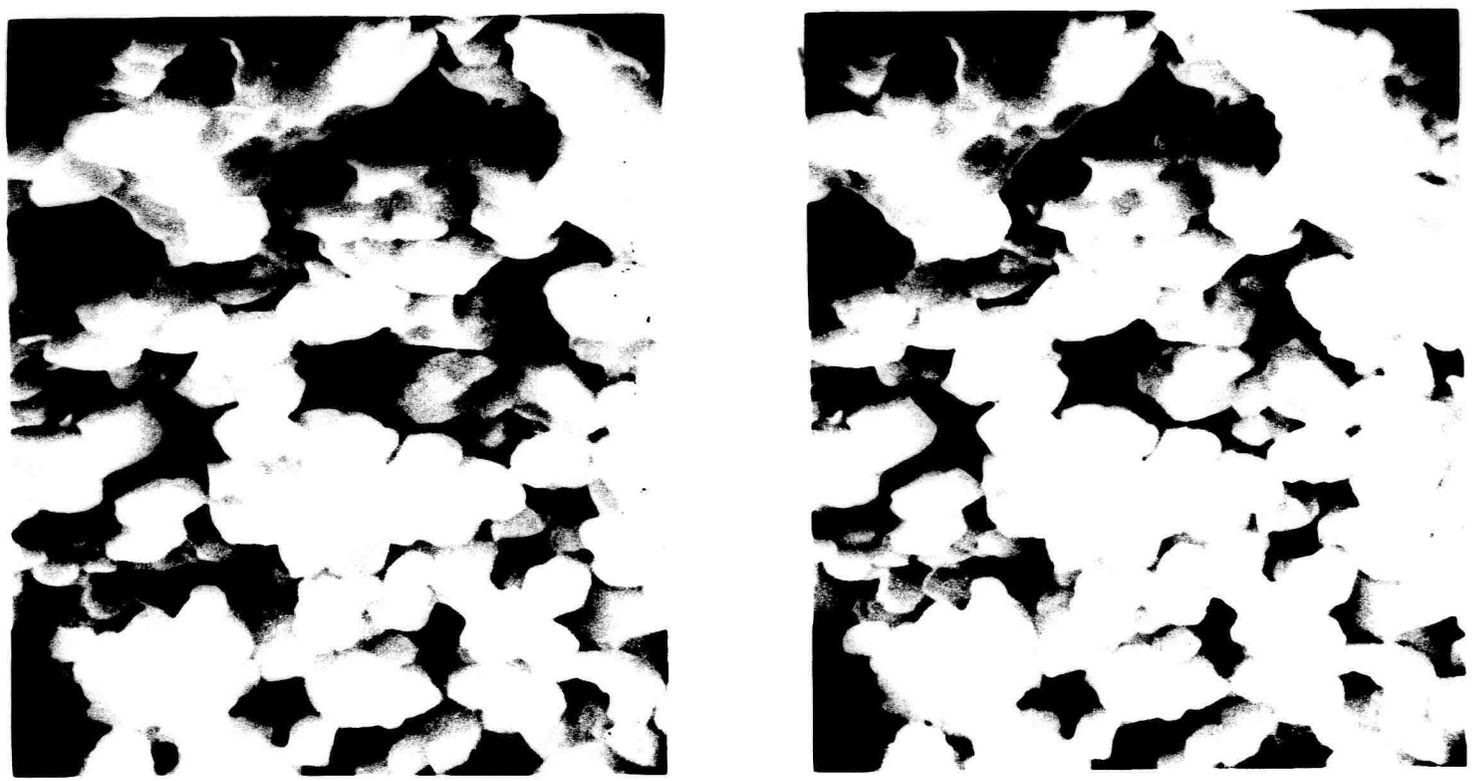

(c) More detail oi the fine interöolite aggregate on the fracture surface. (5000X)

FIGURE 7. STEREO PAIRS OBTAINED BY SCANNING ELECTRON MICROSCOPY OF FRACTURE SURFACE IN SALEM LIMESTONE (Continued).

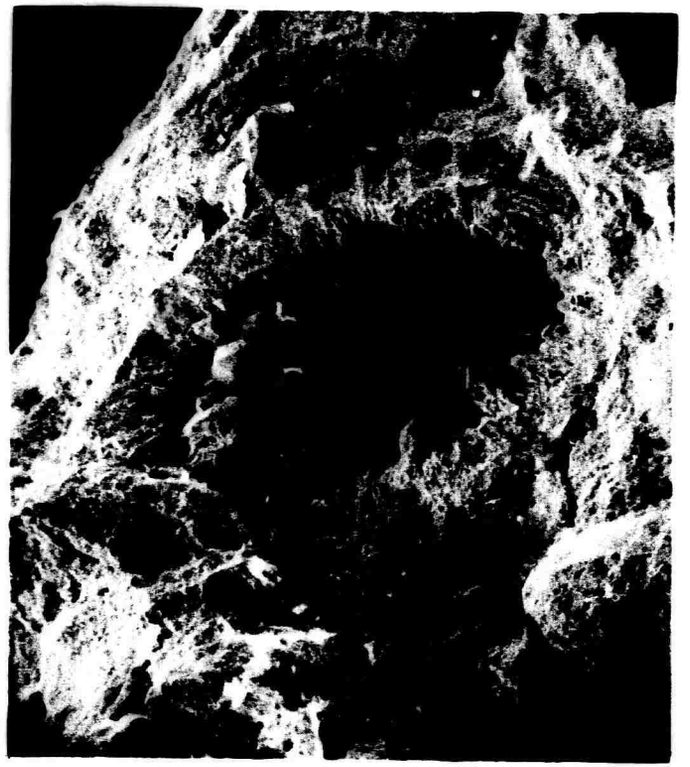

(d) Apparently nearly perfect calcite crystals precipitated within a small cavity which has been broken open during fracturing. (50X)

FIGURE 7. STEREO PAIRS OBTAINED BY SCANNING ELECTRON MICROSCOPY OF FRACTURE SURFACE IN SALEM LIMESTONE (Continued).

limestone, small fragments on the fracture surface were removed and could be observed in the final replica. For example, Figures 8a and 8b show the outlines of numerous micron size particles comprising the matrix, as well as the impression in the replica of areas of the surface. Contrast the irregular character of this surface with the relatively flat cleavage surface of one of the millimeter size particles in Figure 8c. The distinct feature in Figure 7c is known as a river pattern and occurs when the crack passes from one single crystal into another with a very slight difference in crystallographic orientation. It was also discovered that thin flakes of material were removed from these cleavage surfaces. These flakes were thin enough to be transparent to the electron beam thereby revealing the internal structure as can be seen, for example, at ultra-high magnification (108,000X) in Figure 8d. In addition, electron diffraction patterns can be obtained from these flakes, an example of which is shown in Figure 8e. These patterns can be used to make relatively precise determinations of crystal structure. The pattern in Figure 8e has been analyzed and was found to correspond with the structure of single crystal calcite.

Berea Sandstone

A limited number of tests have so far been made on this material. The specimen dimensions and method of testing is identical to that used for the limestone. Because the specimens behaved in a very nonlinear fashion during loading, the determination of R using the derivation described in the Appendix is not correct. The analysis must be modified before reasonably accurate values of R can be obtained. However, the magnitude of R is approximately the same as that obtained for the limestone.

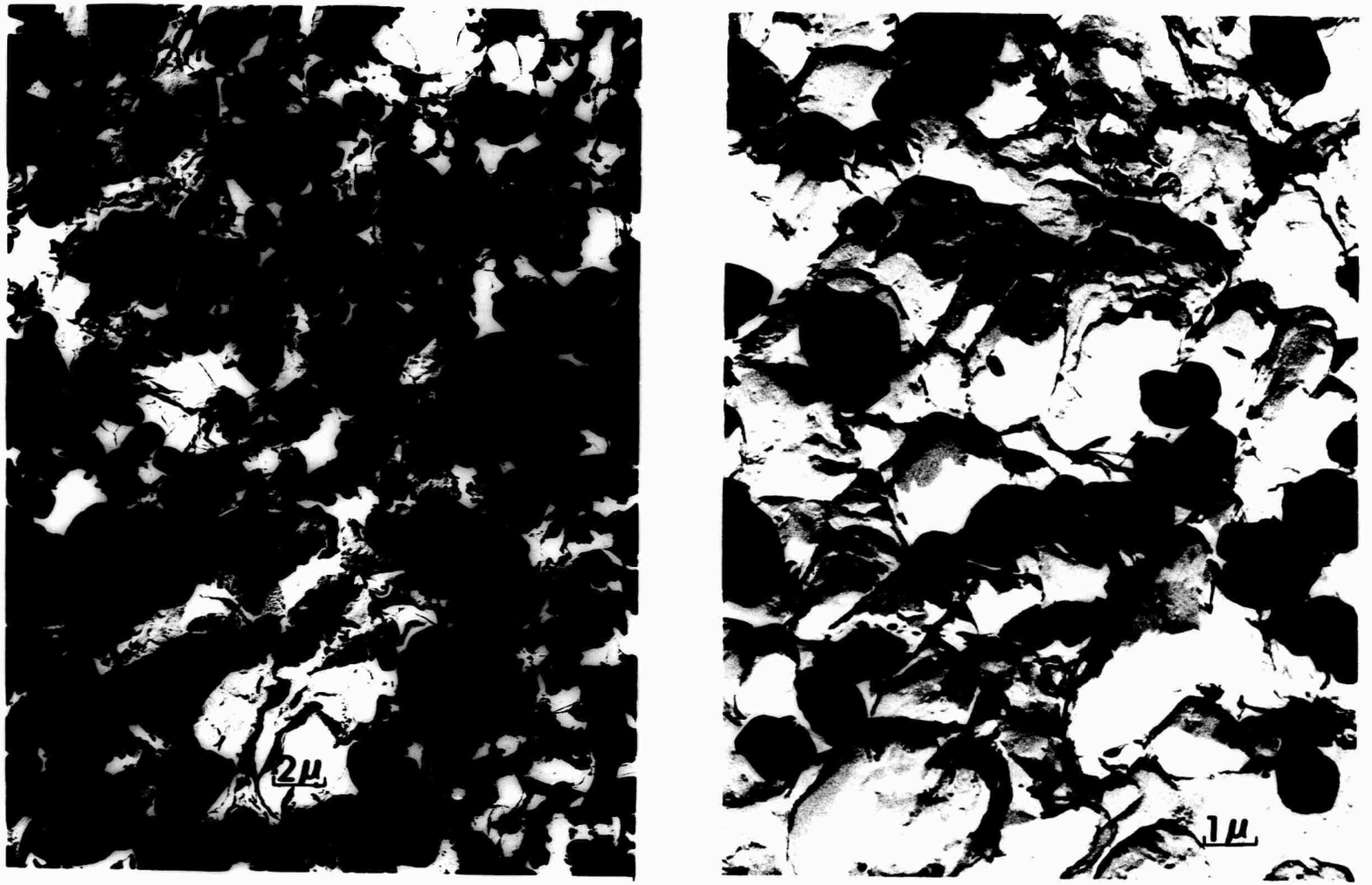

(a) (b)

Micron size interöolite particles extracted from the fracture surface.

FIGURE 8. HIGH RESOLUTION ELECTRON MICROSCOPE FRACTOGRAPHS OBTAINED FROM Pt-C SHADOWED REPLICAS OF THE FRACTURE SURFACE OF SALEM LIMESTONE.

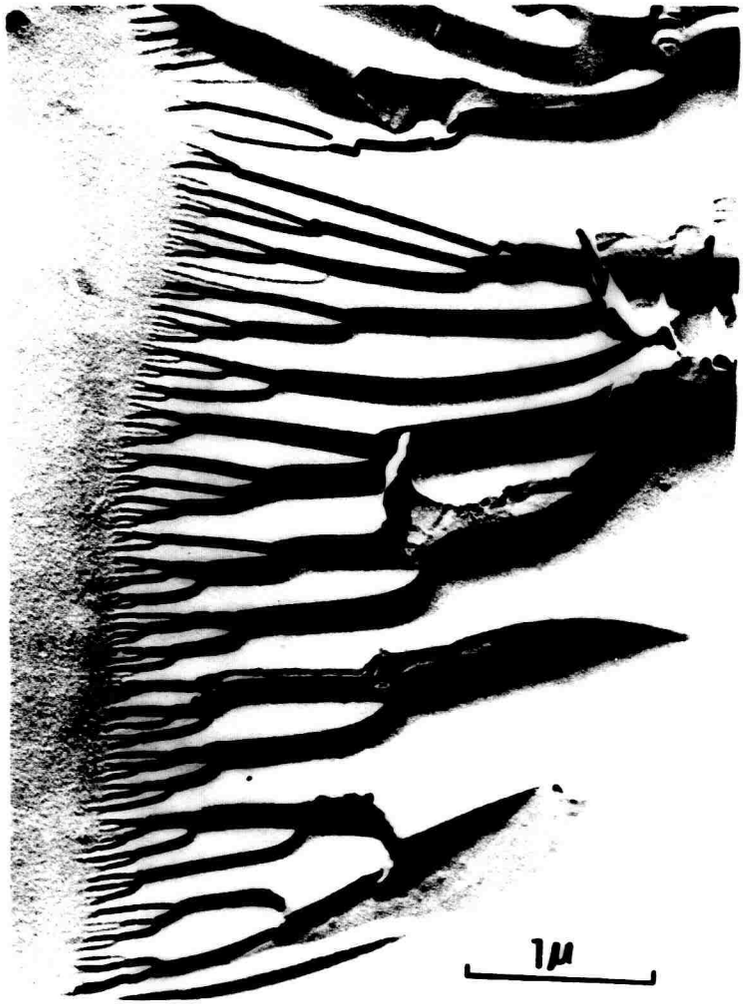

(c) An example of cleavage

(d) A thin flake extracted from a cleavage surface (note that the flake is thin enough to be partially transparent to the beam thereby revealing some internal structure).

FIGURE 8. HIGH RESOLUTION ELECTRON MICROSCOPE FRACTOGRAPHS OBTAINED FROM Pt-C SHADOWED REPLICAS OF THE FRACTURE SURFACE OF SALEM LIMESTONE (Continued).

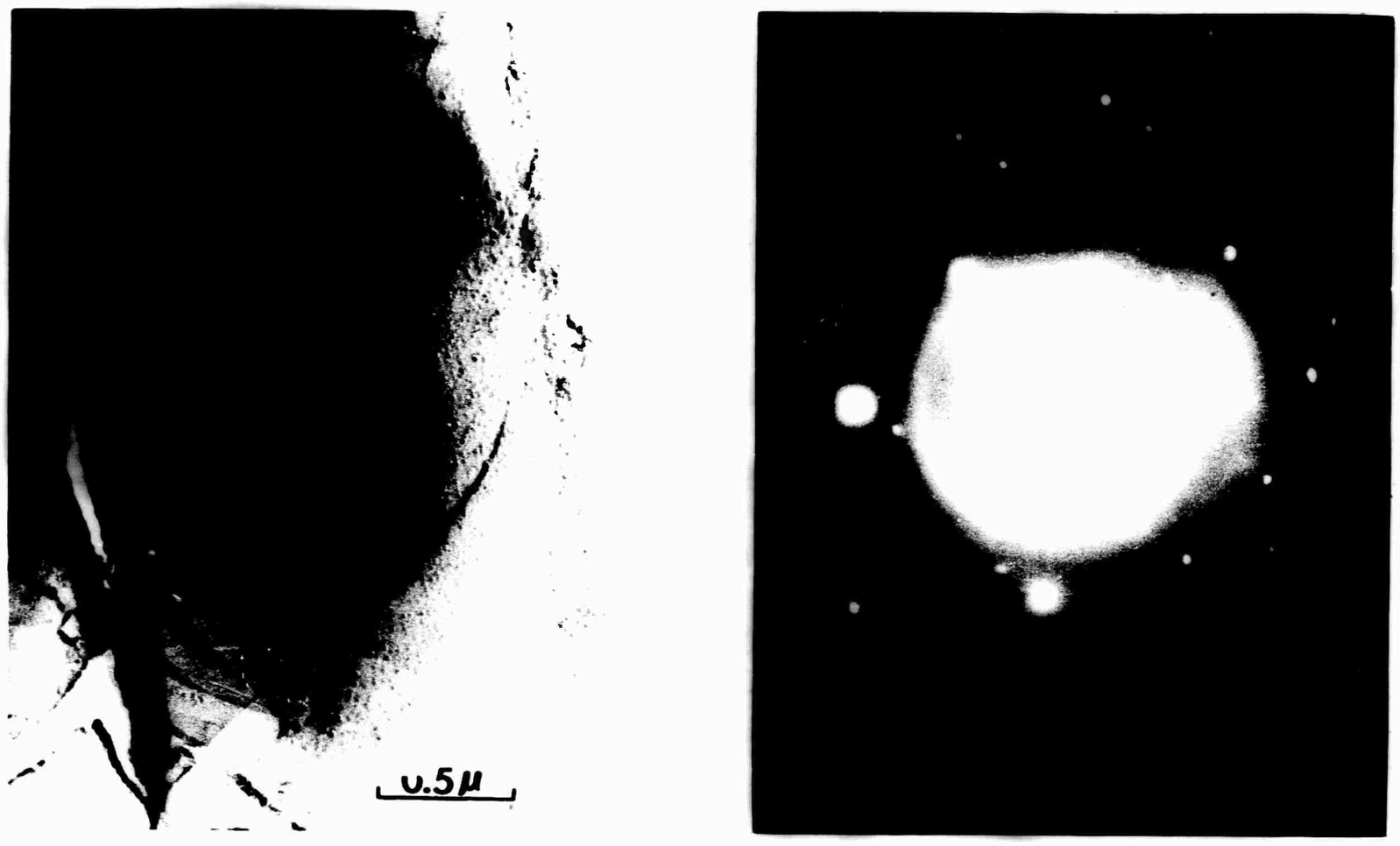

(e) A thin flake extracted from a cleavage surface and the associated electron diffraction pattern.

FIGURE 8. HIGH RESOLUTION ELECTRON MICROSCOPE FRACTOGRAPHS OBTAINED FROM Pt-C SHADOWED REPLICAS OF THE FRACTURE SURFACE OF SALEM LIMESTONE (Continued).

Microstructure

The microstructure consists of remarkably uniform-sized quartz grains (0.3 mm dia.), cemented by calcite. A considerable number of voids are evident and Handin, et al[3] report a volume fraction of pores of 18%. The main crack propagates through the interconnecting calcite layers. Figure 9 provides some evidence that prior to and accompanying the propgation of the main crack there is extensive cracking occurring in a relatively large volume of material adjacent to the crack. During vacuum impregnation of the sandstone, with epoxy resin, penetration was typically only 2-3 mm into the surface. However, around the tip shown in Figure 9 the material is much more permeable as can be seen by the boundary of the epoxy extending farther than 1 cm from the slot tip. Furthermore, during sectioning of specimens containing a crack, it was noticed that quartz grains adjacent to the crack were quite loose and could be easily removed.

Fractography

On the fracture surface at relatively low magnifications, individual quartz grains are readily observable as can be seen on the stereo pairs obtained by scanning electron microscopy in Figure 10a. The grains, which tend to be somewhat elongated exhibit both irregular surfaces and planar facets. There is also some indication here of very narrow cracks in the interfaces between individual grains. At higher magnifications flat areas on which a rather blocky material occurred were observed frequently. The blocky material is likely the broken remnants of the calcite cement or some similar acting material.

Progressing to higher magnifications using electron microscopy of replicas from the fracture surface, two other distinctive features were found.

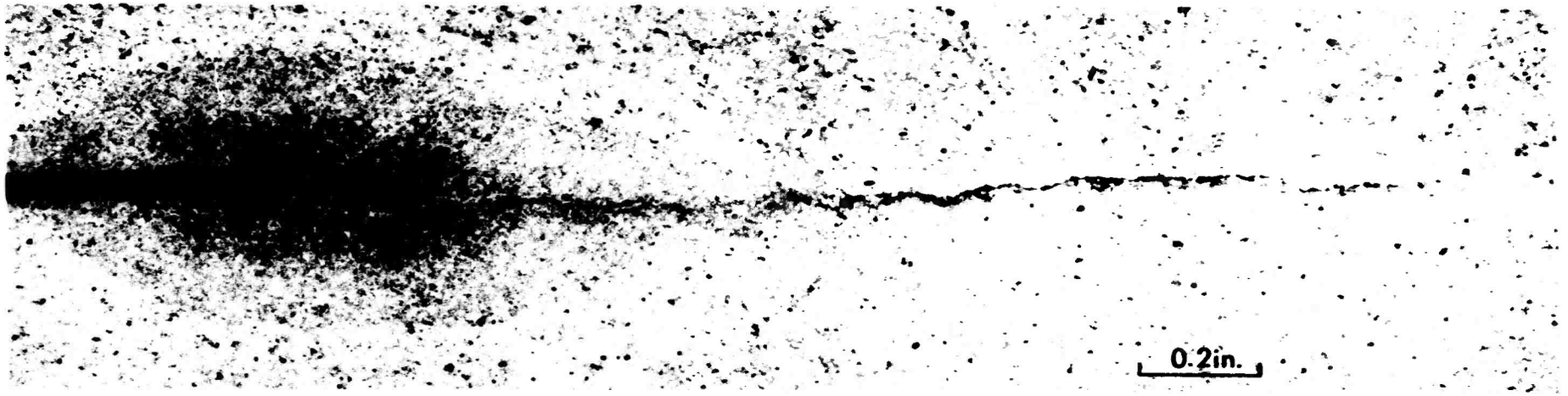

FIGURE 9. CRACK PROFILES AT THE MIDTHICKNESS PLANE OF A BEREA SANDSTONE SPECIMEN. The specimen has been impregnated with an epoxy resin. Note the elliptical zone of penetration of the resin surrounding the slot tip.

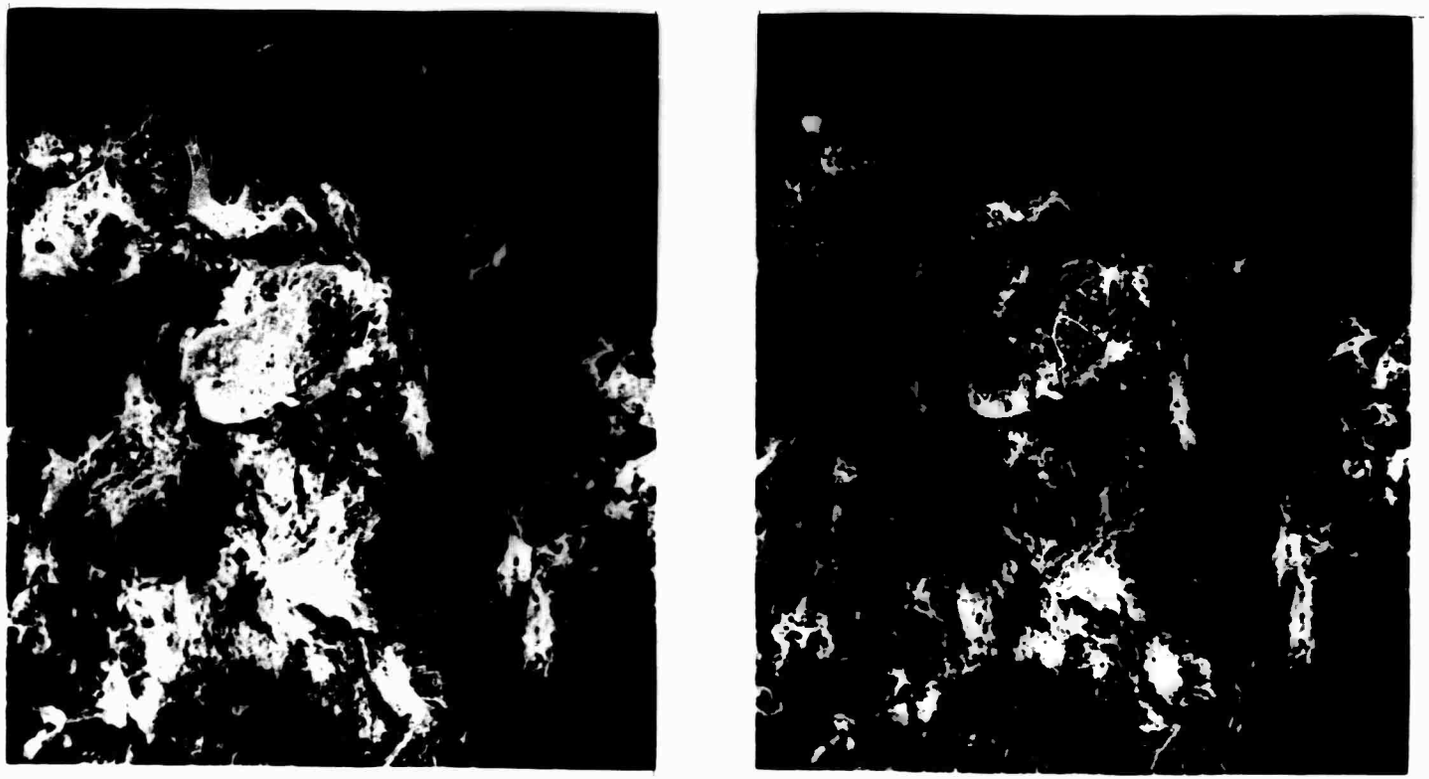

(a)

FIGURE 10. STEREO PAIRS OBTAINED BY SCANNING ELECTRON MICROSCOPY OF THE FRACTURE SURFACE OF BEREA SANDSTONE: (a) low magnification of the fracture surface revealing outlines of the quartz grains (100X) and (b) blocky material adhering to a quartz grain surface (2000X).

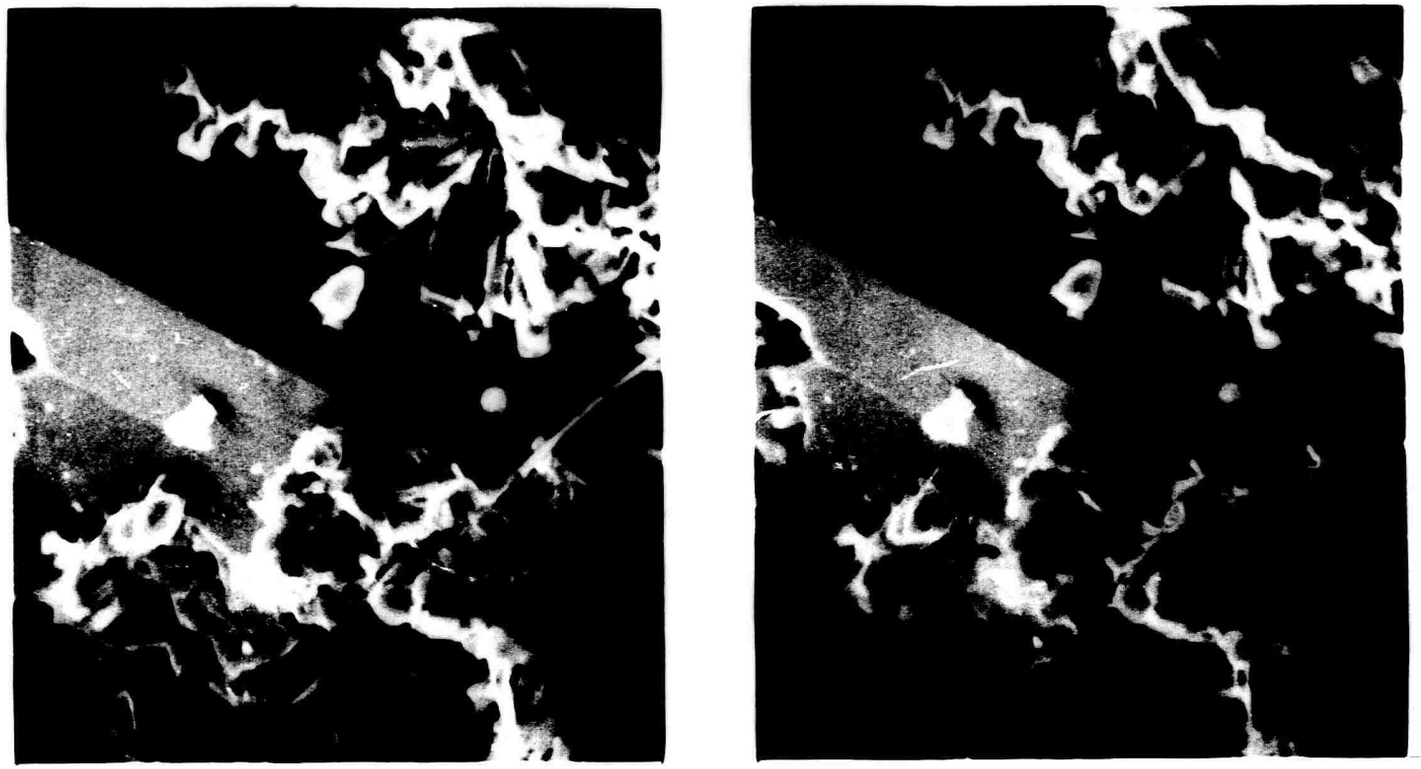

(b)

FIGURE 10. STEREO PAIRS OBTAINED BY SCANNING ELECTRON MICROSCOPY OF THE FRACTURE SURFACE OF BEREA SANDSTONE (Continued).

One of these is a river pattern indication of cleavage and shown in Figure 11a. It can not be firmly established whether these cleavage areas are in the quartz or the calcite but their general appearance is similar to the cleavage morphology found in the limestone, and it is likely that these cleavage areas, which were common on the replicas, predominantly represent the fracture surface of the calcite cement. The other feature commonly observed is shown in Figure 11b and probably is representative of the surface of quartz grains. These blocky crystals exhibit typical habit planes of quartz and are similar to features found on the surface of quartz grains by Kirkpatrick and Summerson[4]. Therefore, these surfaces probably form the pore walls and are not produced as the result of fracture.

Discussion

Using the values of R measured for the limestone, one can obtain an estimate of the tensile strength of this material by applying the simple Griffith theory. The result should not be too much different for the sandstone since crack propagation is through calcite in both cases and furthermore estimates of R which have been made for the sandstone are of the same magnitude as for the limestone. If the rock contains cracks of length (or diameter for penny-shaped cracks), 2a, oriented perpendicular to an applied uniaxial stress then the tensile strength is

$$\sigma_t = \beta\sqrt{\frac{ER}{\pi a}} \qquad (3)$$

where β is a geometry dependent constant of order unity. The following table gives several example tensile strengths for various values of R where

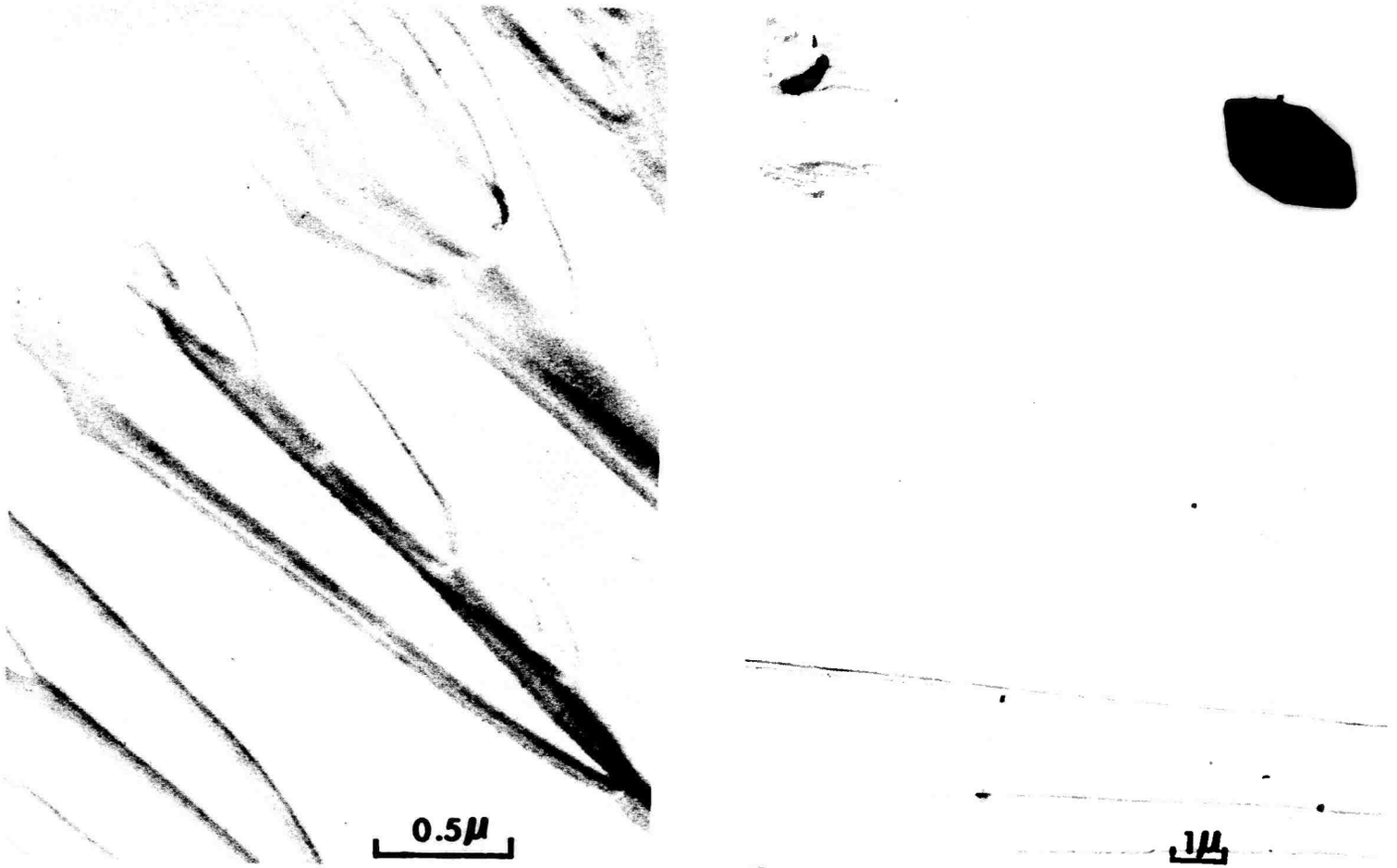

(a)

FIGURE 11. HIGH RESOLUTION ELECTRON MICROSCOPE FRACTOGRAPHS OBTAINED FROM Pt-C SHADOWED REPLICAS OF THE FRACTURE SURFACE OF BEREA SANDSTONE: (a) areas of distinct cleavage and (b) secondary silica deposits.

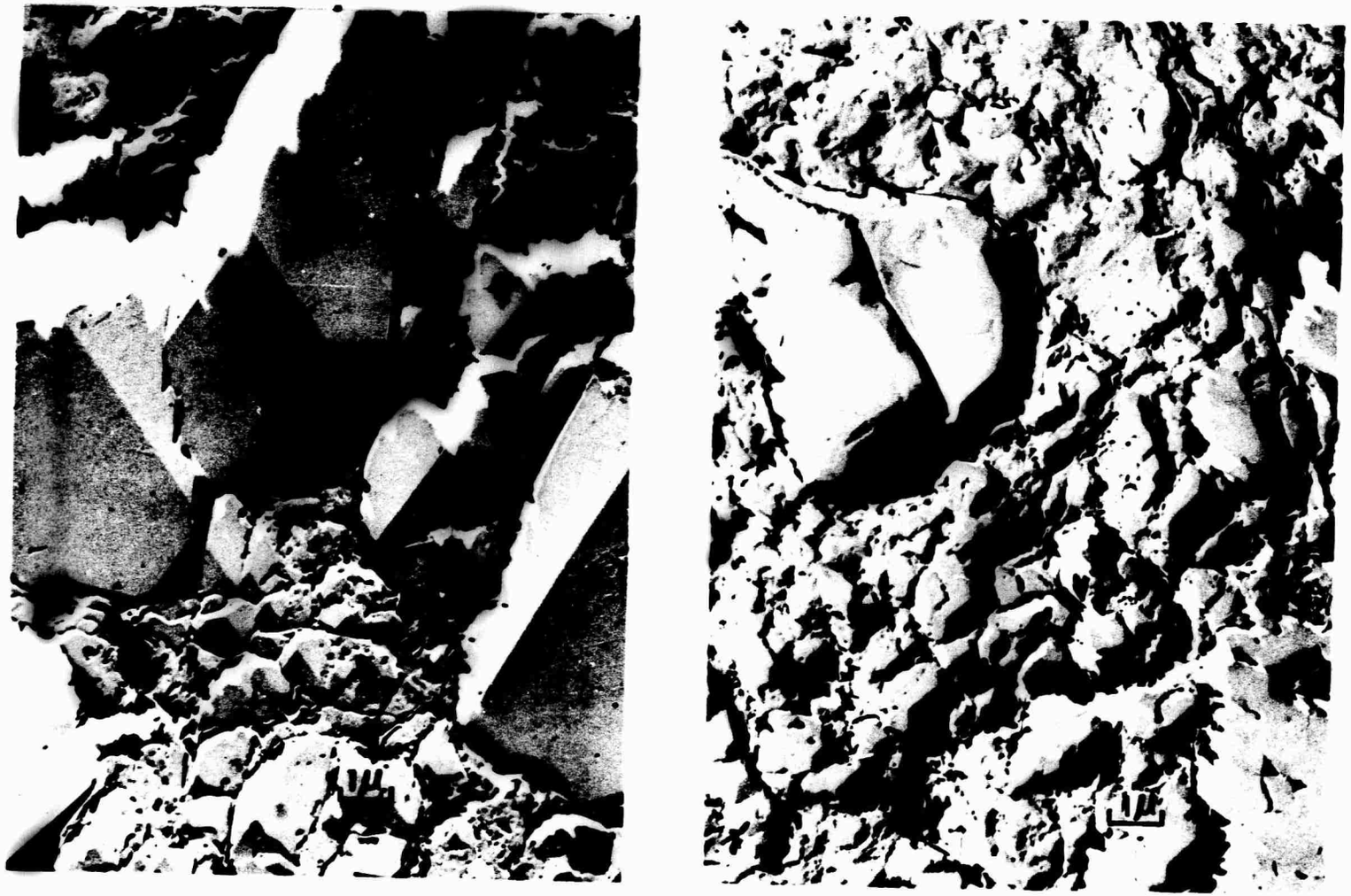

(b)

FIGURE 11. HIGH RESOLUTION ELECTRON MICROSCOPE FRACTOGRAPHS OBTAINED FROM Pt-C SHADOWED REPLICAS OF THE FRACTURE SURFACE OF BEREA SANDSTONE (Continued).

E is taken as 1.6×10^{11} dynes/cm^2 (2.3×10^6 psi) and a is assumed to be 1 mm.

	R	σ_t	
	j/m^2	kg/mm^2	(psi)
(Calculated Examples)	200	3.19	(4630)
	100	2.26	(3280)
	50	1.60	(2320)
	10	0.71	(1040)
	3	0.39	(569)
(Measurements) Reichmuth[5]		0.37	(538)
Gilman[6]	0.46	0.15	(222)

This flaw size is based on the assumption that the largest preexisting flaws have dimensions approximately equal to the grain size. From the R-data obtained in this study, tensile strengths in the range of about 1.0 kg/mm^2 (1450 psi) to 3.5 kg/mm^2 (5070 psi) are predicted for the Salem limestone. For comparison tensile strength data determined by Reichmuth[5] from point load tests of cylinders is given in the table. There is a difference in these results of at least a factor of 3 in σ_t or a factor of 10 in the corresponding R. Alternatively better agreement would be obtained assuming a flaw size of about 2 cm or larger but a preexisting flaw of this dimension seems definitely unrealistic. The intrinsic surface energy (listed here as 2γ) measured by Gilman from single crystal calcite slabs at -196 C is also indicated along with the corresponding predicted value of σ_t for a = 1 mm. Comparing these results, it is evident that it is necessary to not only account for the large differences in predicted and measured tensile strengths but also the rather enormous differences between the intrinsic R for calcite and the R for limestone.

The possible explanations for these differences fall into two categories: (1) irreversible processes are involved in the fracture of the limestone (and sandstone), and (2) the actual crack surface area is larger than the projected surface area ($b\Delta a$). Focusing on possible irreversible processes, it should first be noted that the process of simply forming new surface is reversible and the measurements by Gilman should be close to the reversible energy requirements to form a surface in calcite. Therefore, in the absence of environmental effects, this value represents the smallest possible value of R for propagating a crack in calcite. Irreversible processes leading to the conversion of strain energy into heat which may increase R above this level are plastic deformation (by dislocation motion and twinning) and frictional effects during shear induced sliding. Work done in sliding is likely to be a smaller percentage of the total irreversible losses per unit volume in the DCB tests than in more conventional compression tests because the principal stress components everywhere in the vicinity of the crack tip in the former case are tensile. Furthermore, we have not found evidence of dislocations or a higher twin density at or near the crack plane in the limestone. However, the techniques used may not have been sufficiently sensitive to reveal the presence of these forms of deformation and the loss of energy by irreversible processes can not yet be eliminated.

Alternatively, supposing that the irreversible losses are negligible, then amount of surface area created during the tests on the limestone would necessarily be greater by a factor of from 50 to 500 than the projected surface area. On the other hand Reichmuth's results could be brought into correspondence with Gilman's by assuming a factor of approximately 7. This is not an unreasonable ratio between the actual surface area which is highly irregular and the projected surface area. The increased permeability of the sandstone in the

region surrounding the slot tip and the acoustic activity in the limestone at relatively low loads supports the view that in the DCB tests, a large amount of subsidiary cracking occurs, in effect, creating a "cloud" of numerous small cracks in the volume of material adjacent to the main crack tip. Their creation obviously decreases the stored elastic strain energy in this volume or, equivalently, reduces the stresses. Secondly, their presence reduces the effective bulk properties in this region. The latter effect was discussed previously in regard to uncertainties in the determination of R. Thus, if Young's modulus is decreased then there is a corresponding decrease in the elastic strain energy release rate during growth of the main crack. This effect is reversed in currently accepted tests for measuring tensile strengths such as the Brazilian test or that described by Reichmuth[5]. In these tests one of the principal stresses is a large compression. Accordingly, there is a compaction accompanied by an increase in the effective Young's modulus in the region beneath the point load. It would therefore appear that at least in rocks like limestone and sandstone, that the resistance to crack propagation and, hence the tensile strength, is dependent upon the magnitude of the hydrostatic component of the stress field indirectly as a result of its influence on bulk elastic properties. Similar ideas have been postulated by Jaeger and Cook[7] to explain the effect of stress state on the compressive strength of rocks.

Considering the rather enormous surface area which would be required to bring the measurements of R on the limestone into agreement with the intrinsic R, it seems most reasonable to suggest that the source of R includes irreversible processes as well as subsidiary cracking. However, work remains to be done before the relative roles of these two aspects of tensile fracture in rocks can be made more definitive.

REFERENCES

(1) H. R. Hardy and Y. S. Kim, "Detection of a Low-Level Critical Stress in Geologic Materials Using Ultrasonic Techniques", Proceedings of the Twelfth Symposium on Rock Mechanics, AIME, 1971, p. 301.

(2) T. K. Perkins and L. E. Bartlett, "Surface Energies of Rocks Measured During Cleavage", Soc. Pet. Eng. J., December 1963, p. 307.

(3) J. Handin, R. V. Hager, Jr., M. Friedman, and J. N. Feather, "Experimental Deformation of Sedimentary Rocks Under Confining Pressure", Bull. Am. Assoc. Pet. Geol., 47, 1963, p. 717.

(4) K. T. Kirkpatrick and C. H. Summerson, "Some Observations on Electron Micrographs of Quartz Sand Grains", Ohio J. of Science, March, 1971, p. 106.

(5) D. R. Reichmuth, "Point Load Testing of Brittle Materials to Determine Tensile Strength and Relative Brittleness", Proc. of Ninth Symp. on Rock Mech., AIME, 1968, p. 134.

(6) J. J. Gilman, "Direct Measurement of Surface Energies of Crystals", J. Appl. Phys., 31, 1960, p. 2208.

(7) J. C. Jaeger and N.G.W. Cook, Fundamentals of Rock Mechanics, Methuen and Company, London, 1969, p. 337.

(8) M. F. Kanninen, "An Augmented Double Cantilever Beam Model for Studying Crack Propagation and Arrest", submitted to Intl. J. of Frac. Mech.

(9) R. G. Hoagland, "On the Use of the Double Cantilever Beam Specimen for Determining the Plane Strain Fracture Toughness of Metals", Trans ASME, 89, series D, 1967, p. 525.

APPENDIX

Computation of Energy Dissipation Rates

At the basis of the Griffith energy balance or thermodynamic approach to fracture is the calculation of the stored elastic strain energy in the body given by

$$U = \int_{\tau} \left(\int \sigma_{ij} \, d\epsilon_{ij} \right) d\tau \qquad \text{(A-1)}$$

Here ϵ denotes elastic strain and σ the stress. The subscripts follow the Einstein tensor notation. The outer integral, τ, denotes integration over the volume of the body. The evaluation of U is greatly simplified if there exists a linear (Hookeian) relation between stress and strain throughout the body. Further, the elastic coefficients (Young's moduli) are assumed constant throughout and that the material remains compatible (i.e., no cracks or voids develop). This latter assumption is apparently violated to various degrees in rocks subject to tensile stresses. As a consequence of forming or opening many small cracks, the material becomes more compliant. Equivalently, the bulk elastic properties appear to be reduced. However, within the framework of these assumptions, we can obtain in the case of a DCB specimen, a simple relation between the component of force perpendicular to the crack, P, and displacement, y (between the points of load application):

$$y = \frac{\phi P}{Eb} \qquad \text{(A-2)}$$

where E is Young's modulus, b is specimen thickness, and ϕ is the compliance which depends only on specimen dimensions and crack length. The stored elastic

strain energy also simplifies to

$$U = \frac{1}{2} Py \tag{A-3}$$

and substituting from Equation (A-2)

$$U = \frac{Eby^2}{2\phi} \tag{A-4}$$

The stored elastic energy decreases as the crack extends at a rate given by

$$G = -\frac{1}{b}\frac{\partial U}{\partial a}$$

or

$$G = \frac{E}{2}\left(\frac{y}{\phi}\right)^2 \frac{\partial \phi}{\partial a} \tag{A-5}$$

where G is the elastic energy release rate. If the stored elastic energy is released at the same rate as it is dissipated then G = R and Equation (A-5) is the means of calculating R provided ϕ can be related to crack length. Kanninen[8] has derived this relation and obtains

$$\Phi = \frac{2}{\lambda^3 h^3}\left[2\lambda^3 a^3 + 6\lambda^2 a^2\left(\frac{\text{Sinh}\,\lambda c\,\text{Cosh}\,\lambda c + \sin\lambda c\cos\lambda c}{\text{Sinh}^2\lambda c - \sin^2\lambda c}\right) + \right.$$

$$\left. + 6\lambda a\left(\frac{\text{Sinh}^2\lambda c + \sin^2\lambda c}{\text{Sinh}^2\lambda c - \sin^2\lambda c}\right) + 3\left(\frac{\text{Sinh}\,\lambda c\,\text{Cosh}\,\lambda c - \sin\lambda c\cos\lambda c}{\text{Sinh}^2\lambda c - \sin^2\lambda c}\right)\right] \tag{A-6}$$

$$\lambda = \frac{(6)^{1/4}}{h}$$

$$c = L - a$$

where h is the beam height (one-half the width of the specimen) and L is the specimen length.

Substituting Equation (A-6) into (A-5) gives a means of determining R in terms of the measured displacement y and crack length, a. The displacement is measured at the end of the steel pin blocks (cf., Figure 1). Since the pin blocks have negligible compliance compared to the rock, the point of load application is taken as the interface between the end of the specimen and the pin blocks. The measured displacement is corrected to correspond to the displacement at this point.

As the crack extension was often difficult to measure, the crack length could be obtained indirectly based on the assumption that the coefficient of friction between the wedge and pins remained essentially constant during the test. We have $P = \left(\frac{\partial F}{\partial \psi}\right)_0 F$ where ψ is the compliance relating y to F, the force applied to the wedge, and the above assumption permits us to set $\left(\psi/\phi\right)_0$ constant. This ratio is obtained at the beginning of the test from the slope of the linear portion of the F-y curve (cf., Figure 2) and ϕ which is calculated from Equation (A-6) using the initial slot length. For other values of y and F, the compliance, ϕ, and crack length can be obtained from the following combination of equations:

$$\phi = \left(\frac{\phi}{\psi}\right)_0 \frac{y}{F}$$

and

$$\phi = Aa^n \qquad \text{(A-7)}$$

where A and n are constants. Equation (A-7) is empirical but has been shown to provide a good correlation between the compliance and crack length.[9] The constants A and n are obtained from a least squares fit of Equation (A-6) to Equation (A-7).